

Magnetic Energy Coupling Across Broad Solar Atmospheric Plasma Conditions and Temperature Scales

N. Brice Orange^{1,2}, D. Chesny^{1,3}, and R. Mitchell⁴

¹OrangeWave Innovative Science, LLC, Moncks Corner, SC 29461

²Etelman Observatory, St. Thomas, United States Virgin Islands 00802

³Department of Physics and Space Sciences, Florida Institute of Technology, Melbourne FL 32901

⁴College of Science and Mathematics, University of the Virgin Islands, United States Virgin Islands 00802

Abstract

Investigations of solar variability and its magnetic energy coupling are paramount to solving many key solar and stellar physics problems. Additionally, understanding solar radiation is crucial in elucidating its role in both space weather and the Earth system. Using five years of observations, with coverage of Cycle 24, from the *Solar Dynamics Observatories* Atmospheric Imaging Assembly and Helioseismic Magnetic Imager, radiative and magnetic fluxes, respectively, were measured from coronal hole, quiet Sun, active regions, active region cores, and at full-disk scales. A mathematical formula of temporal thermal variability for our feature set supports a coupling of radiative fluxes, covering large solar atmospheric temperature gradients, with the activity cycle. We present, and mathematically describe, the coupling of radiative fluxes, across broad electromagnetic spectrum regimes, to the available photospheric magnetic energy. This work reveals a potential entanglement of thermodynamic and magnetic energy contributions within previous similar analyses. Our work supports notions to a self-similar central engine of the large scale closed field corona, with potential extension to open field structures at cooler atmospheric layers (i.e., $\log T < 6.0$). Thus, paving the way for improved radiative to magnetic energy coupling descriptions independent of the large scale coronal magnetic field environment, and potentially activity cycle epochs.

Introduction

❖ Variability of extreme-, far-, and ultraviolet (EUV, FUV, and UV, respectively) solar radiation, and its magnetic coupling are paramount to elucidating the nature of coronal heating and quantifying the coupling of the Sun – Earth system (e.g., Barra et al. 2009).

❖ Sun's atmosphere exists in two phases; a magnetically confined phase near the solar surface and an extended phase that interfaces with and comprises the solar wind. The magnetically confined atmosphere can be divided into three distinct regions: active regions (ARs), regions of "quiet" Sun (QS); and coronal holes (CHs).

❖ Radiation emitting plasma structures of these regions dissipate and redistribute solar atmospheric heat and energy, but to date, there exists no general agreement on what mechanism(s) is(are) responsible for converting magnetic energy into heat and transporting it from the chromosphere to the corona (Yurchyshyn et al. 2010), or on the solar atmospheric heights at which this occurs.

❖ Extensive work has been carried out on magnetically confined structures (e.g., Orange et al. 2013; Chesny et al. 2013); works, mainly related to the corona, which have greatly influenced and enhanced our understanding of solar atmospheric heating (e.g., Aschwanden & Nightingale 2005).

❖ Key in pinning down the existence to a single dominant solar/stellar atmospheric heating mechanism of closed magnetic field structures was the linear relationship of coronae X-ray luminosity to photospheric unsigned magnetic flux established by Pevtsov et al. (2003). However, an extension of this work, to date, across broad electromagnetic spectrum and temperature, multiple epochs of solar activity, and with direct comparisons of large scale open to closed magnetic fields remains unexplored.

Observations

❖ **Date:** May 2010 – June 2015, at ~ 5 day intervals.

❖ **Data:** All AIA passbands and HMI LOS magnetograms (Figure 1).

❖ **Features:** Per date, 193 Å imagery utilized to select two CH, QS, ARs, and ARC features (Figure 1).

❖ **Measurements:** Per feature, AIA passbands and HMI magnetograms were utilized to characterize the typical radiative (F_λ) and unsigned magnetic fluxes (B). Similarly, FD characterizations were obtained per date.

❖ **Temporal Variability:** Assessed via,

$$R_\lambda = \frac{F(\lambda, t) - F(\lambda, t_0)}{F(\lambda, t_0)}$$

at running year intervals for each feature. Unsigned magnetic flux variations where handled similarly [i.e., $F(\lambda, t) \rightarrow B(t)$].

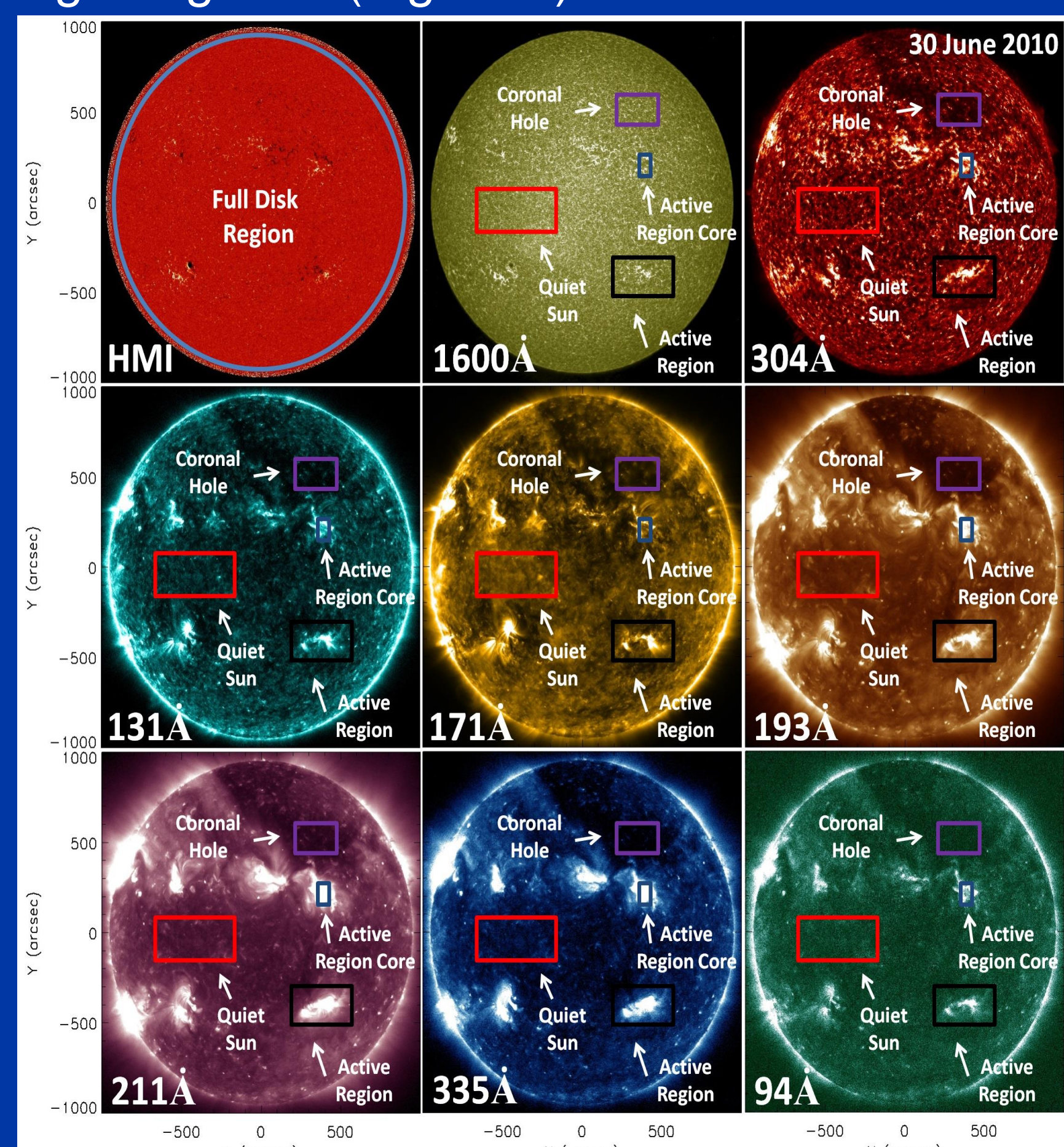


Figure 1. From left to right and top to bottom, respectively, HMI LOS magnetogram, and AIA 1600 Å, 304 Å, 131 Å, 171 Å, 193 Å, 211 Å, 335 Å, and 94 Å radiative images, respectively, observed 30 June 2010. Note, on HMI the circle (blue) indicates the region representing our FD feature, while on each AIA radiative image examples of each of the other gross solar atmospheric feature classes analyzed herein have been identified.

1. Radiative and Magnetic Variations:

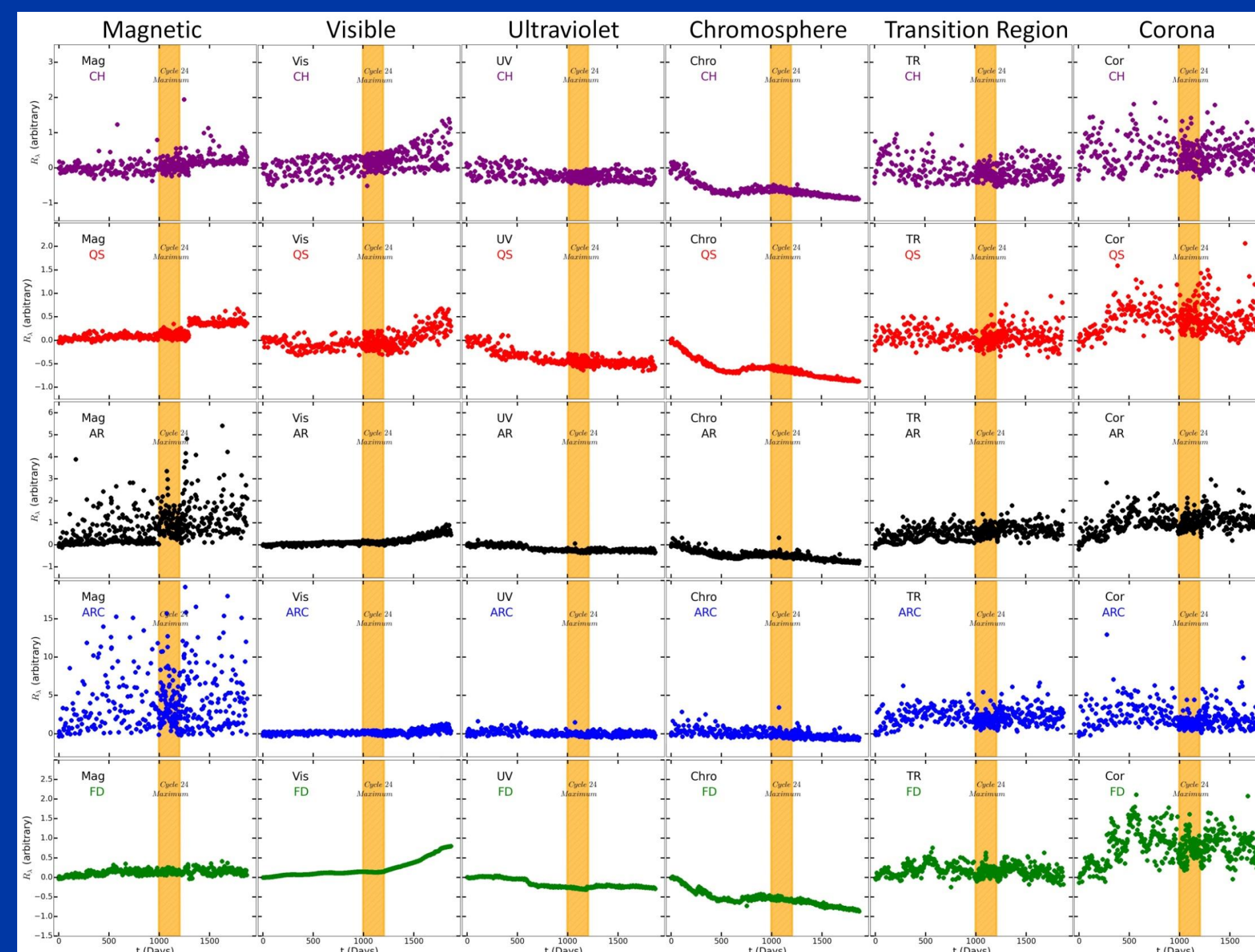


Figure 2. Flux ratios, smoothed over large scale temperature regime, during May 2010 – June 2015, measured relative to May 2010, of magnetic, visible, ultraviolet, chromospheric, TR, and coronal regimes from left column to right column, respectively, for CH, QS, AR, ARC, and FD features from top to bottom row, respectively. Shaded (yellow) region denotes Cycle 24's peak (May 2013 ± 3 months).

2. Running Year R Variations (R')

❖ Our R' results are of distinct interest. In Figure 4, the 2012 – 2013 time interval witnessed a distinct variation from the typical parabolic relationship in temperature found otherwise (times < 2013). Particularly,

$$R_\lambda \propto -\log T^2$$

A trend that continued progressing for study times after the Cycle 24 maximum.

3. Strict Linear: $F_\lambda \propto B^p$

❖ Literature searches provided in Figure (3) as shaded regions.

➤ Consistencies limited to similar studied electromagnetic spectrum, temperature, regimes.

➤ Highlight possible entanglement of thermodynamic and magnetic contributions in previous studies utilizing strict linear relationships (e.g., Pevtsov et al. 2003).

❖ Evidence

➔ Self-similar central engine which breaks down in coronal regimes dominated by single magnetic polarity fluxes

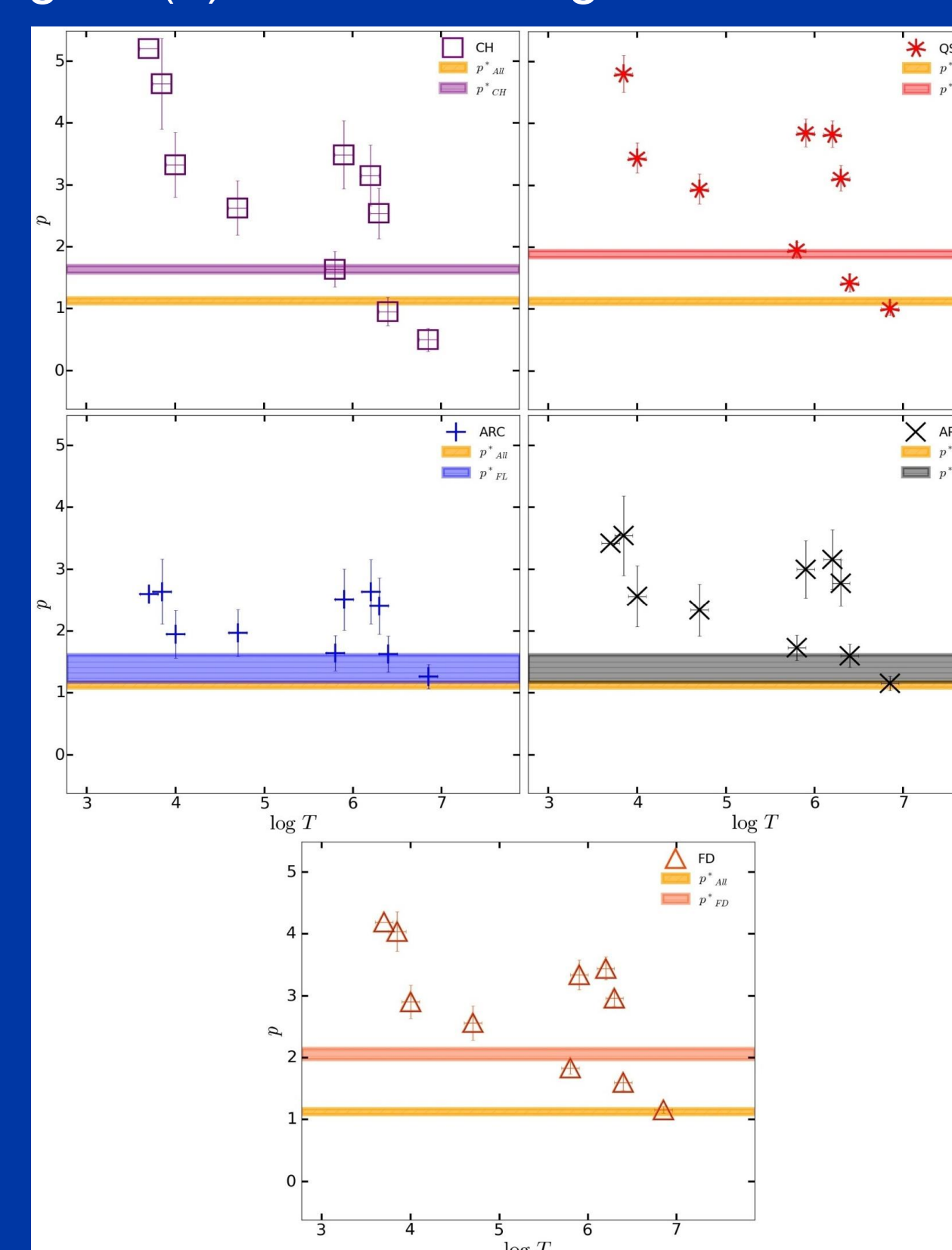


Figure 6. Power-law indices (p) vs temperature ($\log T$) for CH, QS, AR, and FD features denoted by squares (purple), asterisks (red), pluses (blue), x's (black), and triangles (orange), respectively, and from left to right and top to bottom, respectively. Note, shaded, similar color region of each feature denotes power-law indices mined from existing literature, while the shaded (gold) region at $p = 1.13 \pm 0.05$ denotes the overall power-law index reported by Pevtsov et al. (2003).

Acknowledgements

A portion of this research was supported by OrangeWave Innovative Sciences solar physics objective. N. Orange acknowledges the Florida Space Grant Consortium, a NASA sponsored program administered by the University of Central Florida, grant NNX-10AM01H. R. Mitchell acknowledges NSF grant HBCU-UP #1137472. The authors express their gratitude to the University of the Virgin Islands, Dr. D. Morris, and Dr. B. Gendre.

Empirical Results

❖ Ratios vs $\log T$

➔ Similar, parabolic trend independent of feature. Thus, were fitted via

$$R_\lambda = \alpha \log T^2 + \kappa \log T + \gamma$$

where α , κ , and γ are free parameters defined by the MPFIT, for each feature.

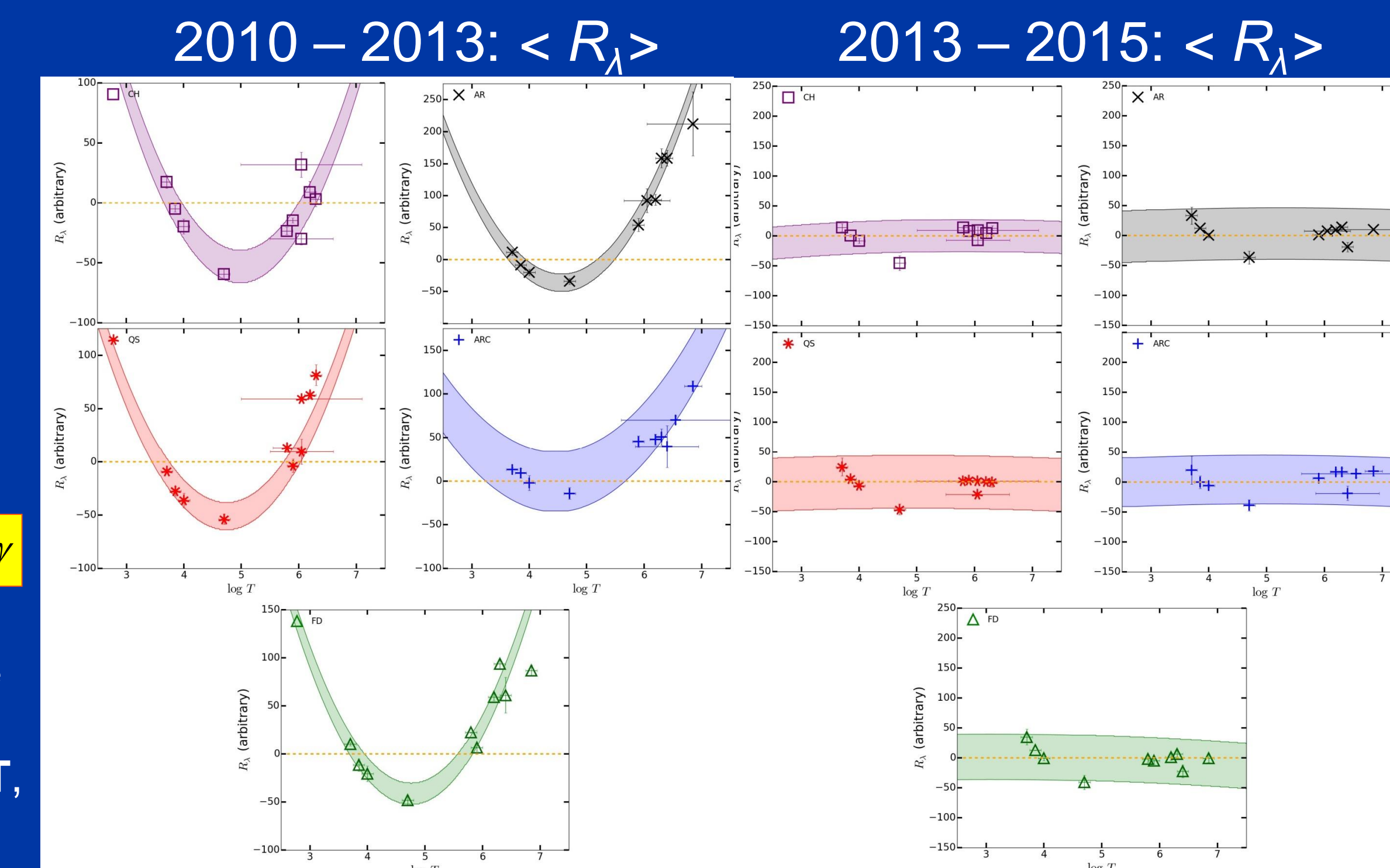


Figure 3. Radiative flux ratios (plotted points), as function of CH (squares, purple), QS (asterisks, red), AR (x's, black), ARC (pluses, blue), and FD (triangles, green) vs temperature ($\log T$) for the 2010 – 2013 (left panel) and 2013 – 2015 (right panel) time frame. Shaded regions on each plot denoted the modeled ratio space derived in this work.

3. Radiative vs Magnetic Flux (2010 – 2013):

❖ Our upper coronal results are consistent with Figure 5b of Benevolenskaya et al. (2002), i.e.,

➔ 2 dependencies of radiative energy versus the underlying magnetic field.

❖ Progressing to cooler layers, results are more consistent with notions of a single linear correlation of radiative to magnetic energy, i.e., Pevtsov et al. (2003).

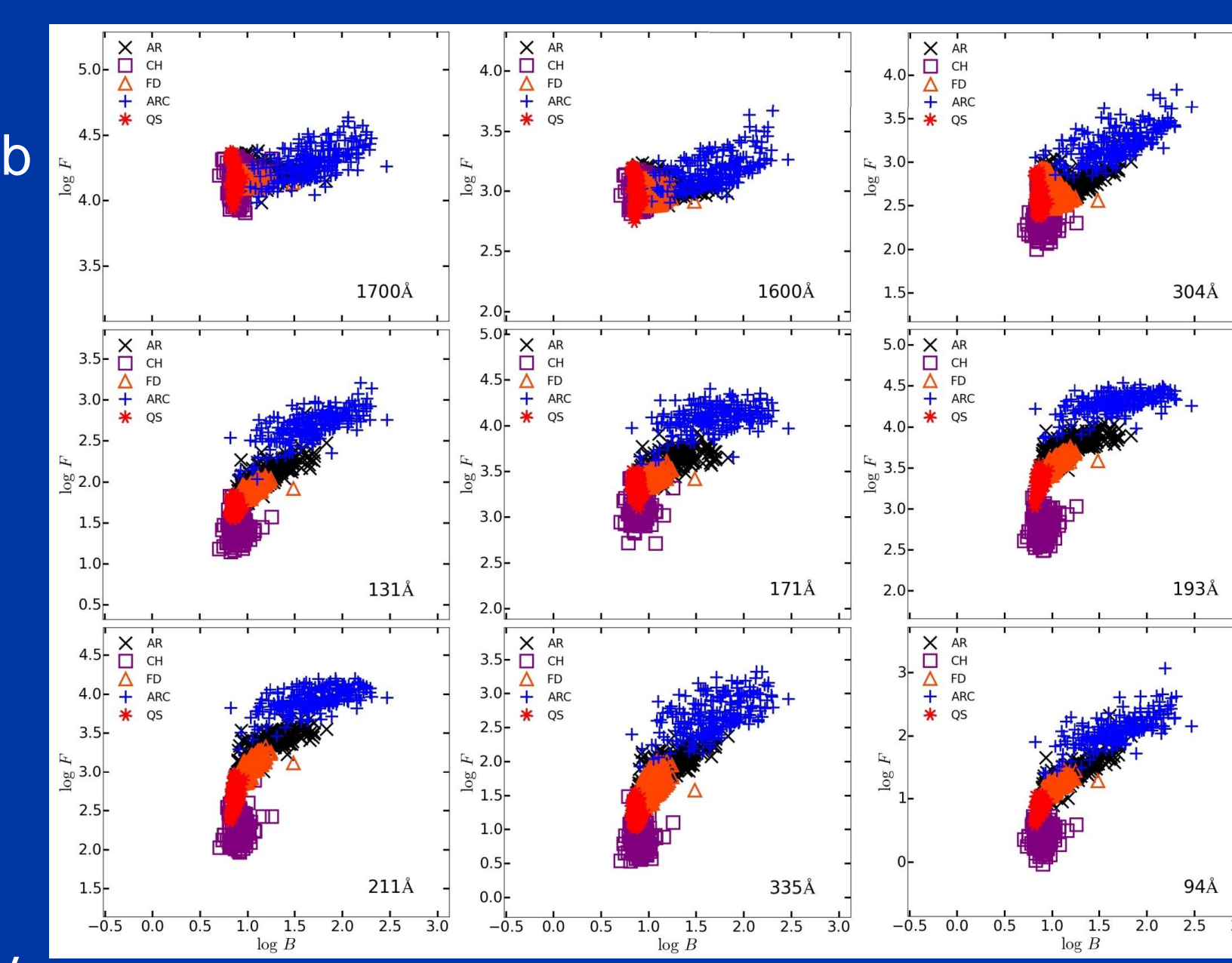


Figure 5. Radiative fluxes (arbitrary units) vs unsigned magnetic flux (arbitrary units) for 1700 Å, 1600 Å, 304 Å, 131 Å, 171 Å, 193 Å, 211 Å, 335 Å, and 94 Å passbands, from left to right and top to bottom, respectively. On each plot CH, QS, AR, ARC, and FD regions are denoted by squares (purple), asterisks (red), x's (black), pluses (blue), and triangles (orange), respectively.

➤ Evidence ➔ Dominant self-similar central engine that clearly breaks down in coronal regimes dominated by single magnetic polarity fluxes

Discussions/Conclusions

❖ Consistent with expectations of single dominant coronal heating mechanism in closed field corona.

❖ Radiative to magnetic energetic descriptions (p) are consistent with literature over similar studied electromagnetic spectrum regimes, i.e., soft X-ray.

❖ Support notions of differing central engines between large scale open and closed magnetic fields; however, for hotter temperature regimes. Additionally, favor the heights of CH formation as cooler atmospheric layers (e.g., Cranmer 2012).

❖ Evidence for an entanglement of thermodynamic and magnetic energy contributions in strict linear analyses; particularly, when assessing large temperature gradients of the solar atmosphere.

❖ Evidence for numerical solar epoch recognition descriptions, across broad electromagnetic spectrum regimes, that emphasize the importance of real time solar monitoring as a tool elucidating the coupled Sun-Earth system details.

References

- Aschwanden, M.J., & Nightingale, R.W. 2005, ApJ, 633, 499
- Barr, V., Delouille, V., Kretzschmar, M., & Hochedez, J.-F., 2009 A&A, 505, 361
- Benevolenskaya, E.E., Kosovichev, A.G., Lemen, J.R., Scherrer, P.H., & Slater, G.L. 2002, ApJ, 571, L181
- Chesny, D.L., Oluseyi, H.M., & Orange, N.B. 2013, ApJ, 778, L17
- Cranmer, S.R. 2012, Space Sci. Rev., 172, 145
- Orange, N.B., Chesny, D.L., Oluseyi, H.M., et al. 2013, ApJ, 778, 90
- Pevtsov, A.A., Fisher, G.H., Acton, L.W., et al. 2003, ApJ, 598, 1387
- Yurchyshyn, V.B., Goode, P.R., Abramenko, V.I., et al. 2010, ApJ, 722, 1970

